ChemPubSoc Europe

DOI: 10.1002/chem.201405792

CHEMISTRY
A European Journal
Full Paper

Oligourea Foldamers

Isosteric Substitutions of Urea to Thiourea and Selenourea in Aliphatic Oligourea Foldamers: Site-Specific Perturbation of the Helix Geometry

Yella Reddy Nelli,[a] Stéphanie Antunes,[a] Arnaud Salaün,[a] Emmanuelle Thinon,[b, d] Stéphane Massip,[c] Brice Kauffmann,[c] Céline Douat,[a] and Gilles Guichard*[a]

Abstract: Nearly isosteric oxo to thioxo substitution was employed to interrogate the structure of foldamers with a urea backbone and explore the relationship between helical folding and hydrogen-bonding interactions. A series of oligomers with urea bonds substituted by thiourea bonds at discrete or all positions in the sequence have been prepared and their folding propensity was studied by using a combination of spectroscopic methods and X-ray diffraction. The outcome of oxo to thioxo replacements on the helical folding was found to depend on whether central or terminal ureas were modified. The canonical helix geometry was not affected upon insertion of thioureas close to the negative end of the helix dipole, whereas thioureas close to the positive pole were found to increase the terminal flexibility and cause helix fraying. Perturbation was amplified when a selenourea was incorporated instead, leading to a structure that is only partly folded.

Introduction

Among the existing approaches to explore the relationship between the structure and function of α-peptides and to improve their resistance to proteolysis, isosteric modifications of the peptide backbone have proven particularly valuable.[1] Many peptide-bond surrogates have been proposed, of which the oxo to thioxo substitution in the peptide bond (Scheme 1 a) is remarkable by several aspects.[1b,2] On one hand, it is one of the most conservative modifications as it preserves both the planarity and the sp^2 hybridization of the amide linkage. On the other hand, the thioamide linkage presents distinct electronic and geometric properties: 1) the C=S bond (1.65–1.68 Å) is longer than the C=O bond in amides, 2) the weaker hydrogen-bond acceptor ability of sulfur and the increased hydrogen-bond donor ability of the more acidic thioamide NH group, 3) the shorter C–N bond length and the higher C–N rotational barrier, 4) the higher dipole moment, 5) the reversible *cis*/*trans* isomerization upon UV irradiation.[3] Altogether, the specific features of the thioamide linkage[4] make it useful as a tool to modulate the (bio)activities of a peptide,[5] as a probe to site specifically perturb and study peptide secondary structures including helices and β-sheets,[5d,6] as a biophysical tool to monitor protein folding and protease activity upon fluorescence quenching,[7] as a photoswitch,[8] as well as a probe of the helical screw sense preference in helical peptides.[9] Some of these physicochemical properties (C–N rotation barrier, electronic excitation energy, dipole moment, and p*K*a value) have been shown to be linearly correlated with the chalcogen polarizability (i.e., O < S < Se).[10] Cognate selenoxo peptides whose synthesis has been achieved recently, display *cis* to *trans* photoisomerization properties at higher wavelength and have been used successfully as photoswitches to control the peptide backbone conformation.[10,11]

Thioamide replacements have also been employed in the context of β-peptide[12] and peptoid chemistries to gain additional insight into the folding propensities of these non-natural oligoamides (e.g.. the 3_{14} helix of β-peptides) and/or to stabilize alternative conformations (e.g., the *cis* conformer in peptoids).[13,14] In this work, we propose to use the oxo to

[a] *Dr. Y. R. Nelli,[+] S. Antunes,[+] Dr. A. Salaün, Dr. C. Douat, Dr. G. Guichard*
Université de Bordeaux, CNRS
Institut Polytechnique de Bordeaux
UMR 5248 CBMN
Institut Européen de Chimie et Biologie
2 rue Robert Escarpit, 33607 Pessac (France)
E-mail: g.guichard@iecb.u-bordeaux.fr

[b] *Dr. E. Thinon*
CNRS, Institut de Biologie Moléculaire et Cellulaire
Laboratoire d'Immunopathologie et Chimie Thérapeutique
15 rue René Descartes, 67084 Strasbourg (France)

[c] *S. Massip, Dr. B. Kauffmann*
Université de Bordeaux, CNRS
UMS 3033, INSERM US001
Institut Européen de Chimie et de Biologie
2 rue Robert Escarpit, 33607 Pessac (France)

[d] *Dr. E. Thinon*
Present address:
Laboratory of Chemical Biology and Microbial Pathogenesis
The Rockfeller University,
1230 York Avenue, Box 250, New York NY 10065 (USA)

[+] *Y.R.N. and S.A. contributed equally to this work.*

Supporting information for this article is available on the WWW under http://dx.doi.org/10.1002/chem.201405792.

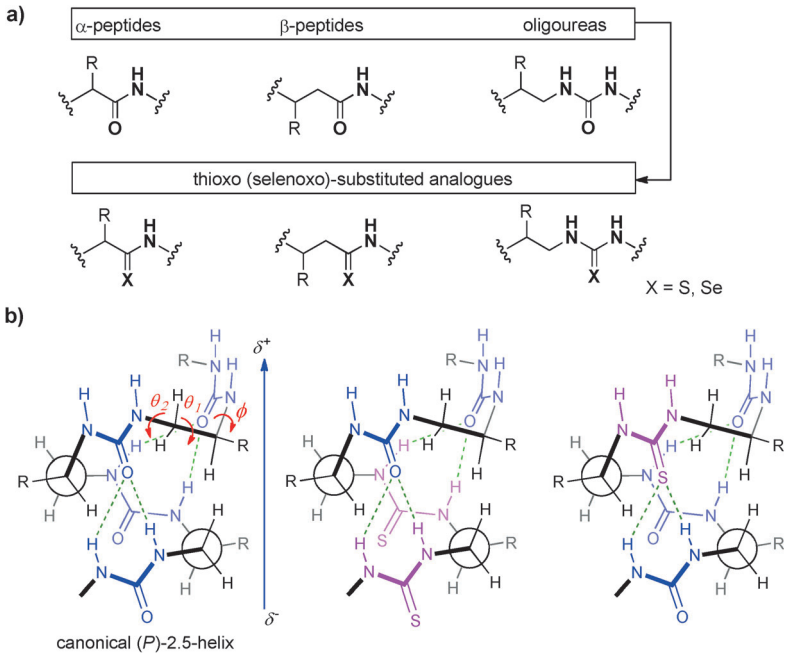

Scheme 1. a) Oxo to thioxo replacement in α- and β-peptides and aliphatic *N,N'*-linked oligoureas. b) Schematic representation of the polar helical secondary structure of oligoureas and of the main-chain thiourea modifications showing how the position of a thiourea in the sequence will affect differentially the hydrogen-bond network.

thioxo (or selenoxo) substitution to interrogate the structure and function of foldamers[15] made of urea linkages instead of amide bonds.[16,17]

Oligoureas consisting of chiral ethylene diamine units connected by a carbonyl group are known to adopt a regular helical structure (2.5-helix) maintained by a network of three centered hydrogen bonds closing 12- and 14-membered pseudocycles.[18] The significant differences between ureas and thioureas in terms of the conformational behavior and the hydrogen-bonding preferences have been largely exploited in the fields of crystal engineering,[19] anion recognition, sensing and transport,[19,20] as well as organocatalysis,[21] but not in foldamer chemistry thus far. The increased acidity of the thiourea NH groups (−6 p*K*a units)[22] is expected to contribute to the oligourea helix stabilization by increasing the strength of the intramolecular hydrogen-bonding interactions. In contrast, the metrics of hydrogen bonding to C=S (and C=Se) acceptors differ significantly from that to C=O (i.e., lower directionality of C=S···H bonds resulting from a more diffuse lone pair density as well as increased hydrogen-bond length),[19,23] suggesting that thioxo (and selenoxo) substitution(s) may cause significant (local) perturbation of the intramolecular hydrogen-bond network in the helical structure of oligoureas and thus local conformational rearrangements. In this work, positional thiourea scanning was used to examine the relationship between the helical folding and the hydrogen-bonding interactions in oligourea foldamers (Scheme 1 b). A series of oligomers with urea bonds substituted by thiourea (or selenourea) at discrete or all positions in their folding propensity investigated systematically by using a combination of spectroscopic methods (NMR, electronic circular dichroism (ECD), and FTIR) and X-ray diffraction analysis.

Results and Discussion

Design and synthesis of oligo(thio)ureas

Oligoureas form a polar helical structure with the urea groups oriented parallel to the helix axis. Depending on their position in the sequence, the main chain ureas contribute differently to the intramolecular hydrogen-bonding network stabilizing the helix (Scheme 1 b). Both the NH and the carbonyl groups of the central ureas are involved in complementary and directional intramolecular hydrogen-bonding interactions. In contrast, the carbonyl groups of the two terminal residues close to the negative pole of the helix, and the NH groups of the two terminal ureas at the positive pole of the helix point towards the solvent and do not form any intramolecular hydrogen bond.

Thus, the outcome of oxo to thioxo replacements on helical folding/unfolding will likely depend on whether central or terminal ureas are modified. The *N*-*tert*-butyloxycarbonyl (Boc)-protected hexamer **1** containing aliphatic side chains (Me, *i*Pr, and *i*Bu) and a terminal Boc protecting group was selected as a model helical oligourea for studying the effects of urea to thiourea replacements (Scheme 2). Urea oligomers such as hexamer **1** have been shown previously to adopt a well-defined helical secondary structure in polar solvents (MeOH, 2,2,2-trifluoroethanol (TFE)).

A series of related oligo(urea/thiourea) hybrids **2**–**5** containing either one or two consecutive thiourea substitution(s) at the terminal positions (compounds **2** and **5**) or in the center of the sequence (compound **3** and **4**) have been prepared for conformational investigation (Scheme 2). One analogue of compounds **1** and **5** in which the last (thio)urea bond close to the positive pole of the helix was substituted for a selenourea (i.e., compound **6**) was also considered to evaluate the effect of the even longer selenoxo bond (C=Se bond length ≈ 1.85 Å) on the hydrogen-bonding interactions in the helix. Finally, the fully thiourea homooligomer analogue of compound **1** containing six thiourea linkages (i.e., compound **7**) has also been prepared for direct comparison with hexamer **1**. All oligomers were synthesized in solution by using activated (*S*)-succinimidyl-{2-{[(*tert*-butoxy)carbonyl]amino}-2-X-ethyl}carbamate monomers for the introduction of urea bonds as previously described.[24] The related thiocarbamoylbenzotriazole derivatives **9** used as masked isothiocyanates for the insertion of thi-

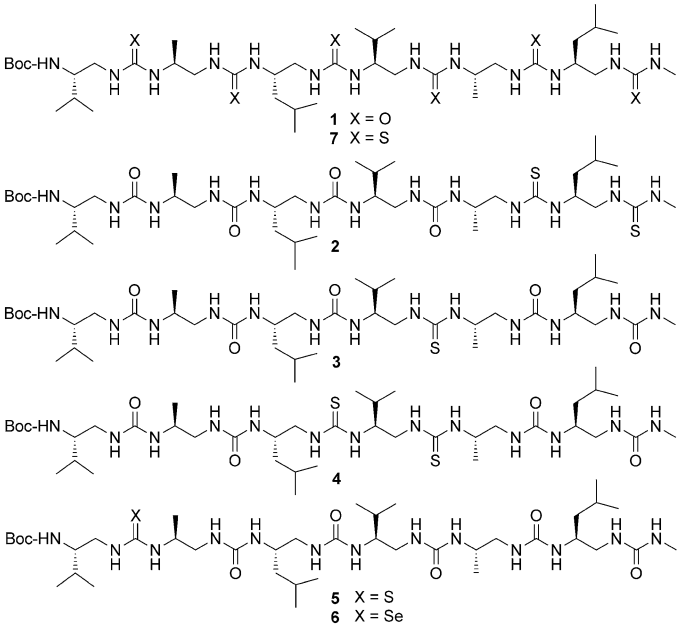

Scheme 2. Formulae of the oligourea **1**, the cognate oligo(urea/thiourea) hybrids **2**–**5**, the oligo(urea/selenourea) hybrid **6**, and the thiourea homooligomer **7**.

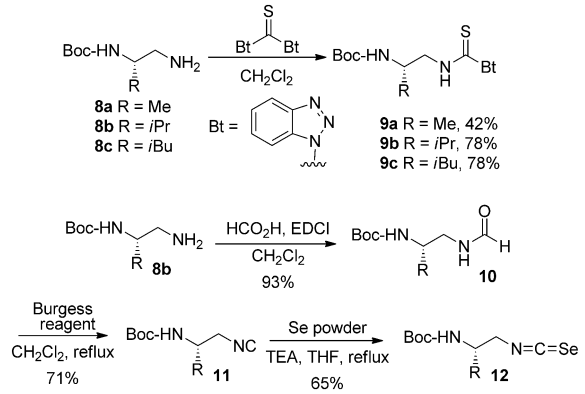

Scheme 3. Synthesis of the activated thiocarbamoylbenzotriazole derivatives **9** used for the introduction of the thiourea units in oligomers **2**–**5** and **7** and of the known isoselenocyanate **12**[27] for the installation of the selenourea unit in **6**. Bt = benzotriazolyl, EDCI = 1-ethyl-3-(3-dimethylaminopropyl)-carbodiimide, TEA = triethylamine.

ourea units were readily obtained by activation of the *N*-Boc-protected ethylene diamine derivatives **8** with bis(benzotriazolyl)methanethione (Scheme 3).[25] Isothiocyanates derived from monoprotected diamines have also been employed for the synthesis of short thiourea-containing oligomers.[26]

For the introduction of the selenourea unit in compound **6**, we used the known isoselenocyanate **12**[27] prepared in four steps from the *N*-Boc-protected diamine **8b**. The diamine was first converted to the corresponding formamide **10**, which was subsequently dehydrated to isonitrile **11** with the Burgess reagent and transformed to the isoselenocyanate by treatment with Se powder in an overall yield of 43% (Scheme 3).

Positional thiourea scan and conformational analysis of the oligomers 2–5

Characterization of the oligo(urea/thiourea) hybrids **2**–**5** in solution and comparison with compound **1** was first carried out by using electronic circular dichroism (ECD) and FTIR spectroscopy. It is now well established that *N*,*N*′-linked oligoureas such as compound **1** display a characteristic ECD signature upon (*P*)-2.5-helix formation with a maximum of positive molar ellipticity $[\theta]$ at around 203 nm and a negative band with a weaker intensity at 188 nm.[18d,28] These two bands may be due to exciton splitting of the π–π^* transitions in the urea chromophore. Only few studies have examined the chiroptical properties including the ECD spectra of simple thioureas.[29] For example, the UV and ECD spectra of 1,1′-((1*S*,2*S*)-cyclohexane-1,2-diyl)bis(3-methyl)thiourea are dominated by π–π^* transitions polarized parallel (240–250 nm) and perpendicular to the chromophore symmetry axis (210 nm).[29b] The different oligo(thio)urea hybrids were thus expected to give rise to characteristic but more complex ECD signatures because of the presence of two different chromophores and of possible exciton Cotton effects arising from both coupling between identical and different chromophores through space.

The ECD spectra of compounds **1**–**5** measured at a concentration of 2×10^{-4} M in 2,2,2-trifluoroethanol are shown in Figure 1. The characteristic Cotton effects at approximately 188

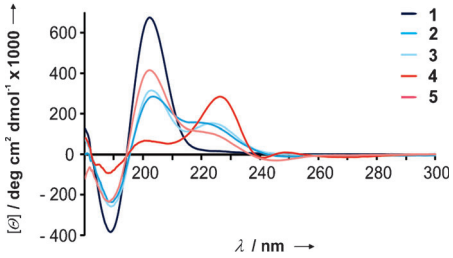

Figure 1. ECD spectra of oligomers **1**–**5** in TFE (2×10^{-4} M) at 298 K.

(negative) and 203 nm (positive) typically assigned to the helical conformation of homooligoureas are detected in the spectra of all hybrid oligomers, though with smaller intensities compared to compound **1**. The ratio of their molar ellipticity $[\theta_{188}]/[\theta_{203}]$ varies from 0.5 for compound **5** to 1.34 for compound **4** ($[\theta_{188}]/[\theta_{203}] = 0.57$ for compound **1**). An important feature of the spectra of hybrids **2**–**5** is the presence of a second positive band at 225 nm that is likely to result from homochromophoric or bichromophoric coupling of the π–π^* thiourea transitions. The relative intensity of the two bands at 203 and 225 nm ($[\theta_{203}]/[\theta_{225}]$) varies among the hybrids from 0.24 in compound **4** to 4.8 in compound **5**. The replacement of two consecutive ureas by thiourea units in the central part of the helix has the most significant impact on the original CD signature of the helical oligoureas with only a weak remaining contribution of the signals at 188 and 203 nm and a strong signature of the thiourea π–π^* band at 225 nm.

Table 1. C=O and C=S stretching frequencies for oligomers **1**–**6** in solution and solid state.

Compd.	Solution[a]		Solid state[a]	
	urea I	urea II	urea I	urea II
1	1639 (s)	1583 (m), 1557 (sh)	1635 (s)	1577 (m), 1556 (sh)
2	1639 (s)	1576 (m), 1559 (sh)	1642 (s)	1576 (m), 1548 (sh)
3	1643 (br)	1582 (m), 1560 (w, sh)	1642 (br)	1575 (br), 1549 (w, sh)
4	1654 (br)	1576 (br), 1562 (w, sh)	1646 (br)	1569 (br), 1544 (w, sh)
5	1645 (br)	1577 (br), 1559 (w, sh)	1636 (m)	1573 (m), 1546 (sh)
7	–	1576, 1560 (br)	–	1574, 1556 (br)

[a] Spectra recorded in MeOH (1–2 mg mL^{-1}). Abbreviations: s = strong absorption, m = medium absorption, br = broad, sh = shoulder, w = weak.

FTIR analysis of oligourea **1** and the thiourea derivatives **2**–**5** was conducted in solution and on the powder (see Figures S50 and S51 in the Supporting Information). The main bands observed in the characteristic $\tilde{\nu}=1400$–1800 cm^{-1} region are collected in Table 1. We have previously shown that the FTIR spectra of helically folded homooligoureas are dominated by two strong and sharp bands centered near $\tilde{\nu}=1635$ and 1580 cm^{-1}. These two bands, which are essentially due to carbonyl stretching and to the coupled C–N stretching/N–H deformation are referred to as "urea I" and "urea II", respectively, by analogy to the amide I and amide II bands in peptides and proteins.[18a,30] The vibrational spectroscopy characterization of thiourea and numerous thiourea metalo complexes reported in the literature provide some hint about the contribution of the thiourea moieties to the FTIR spectra of hybrid oligomers.[31] For thiourea, the $\tilde{\nu}=1400$–1700 cm^{-1} region is dominated by several bands that have been assigned to symmetric and asymmetric N–H bending ($\tilde{\nu}\approx1600$ cm^{-1}) and C–N stretching ($\tilde{\nu}\approx1450$ cm^{-1}) vibrations.

The FTIR spectrum of oligourea **1** recorded in methanol (1 mg mL^{-1}) exhibits two intense "urea I" and "urea II" bands at $\tilde{\nu}=1639$ (sharp) and 1583 cm^{-1} (broader), respectively, which is consistent with helix formation. It is noteworthy that a very similar spectrum was also observed for hybrid **2** with the presence of an intense and sharp band at $\tilde{\nu}=1639$ cm^{-1} that may also indicate a helical conformation. Very similar spectra were measured on the powder. Although dominated by two main bands at similar wavelengths, the solution FTIR spectra of the hybrid hexamers **3**–**5** differ significantly from that of compound **1**. The "urea I" band in these spectra is weaker, significantly broader and is shifted towards higher wavelengths in solution (Table 1). This modification of the FTIR signature and mainly of the "urea I" band reflects a modification of the canonical hydrogen-bonded scheme resulting from thiourea insertion in these oligomers.

The consequences on the 2.5-helix conformation of oligoureas of discrete oxo to thiooxo replacements was also studied in more detail by ^{1}H NMR spectroscopy in CD_3OH (sample concentration 5 mM). Proton resonances were assigned by using homonuclear COSY, TOCSY, and ROESY 2D experiments (Tables S1–S5 in the Supporting Information). Unequivocal sequence-specific assignment was accomplished by analysis of short-range N′H(i)/NH(i+1) rOe connectivities in the ROESY spectra. The signals of the thiourea NHs ($\delta=7.1$–8.0 ppm) appear systematically downfield to the corresponding urea NHs ($\delta=5.7$–6.7 ppm) thus facilitating assignment of all proton resonances and of the rOe connectivities.

However, thiourea NHs were found to display consistently broader signals than that of urea NHs, that may be indicative of a slow chemical exchange resulting from *Z*–*E* rotameric interconversion (Figure 2).[32]

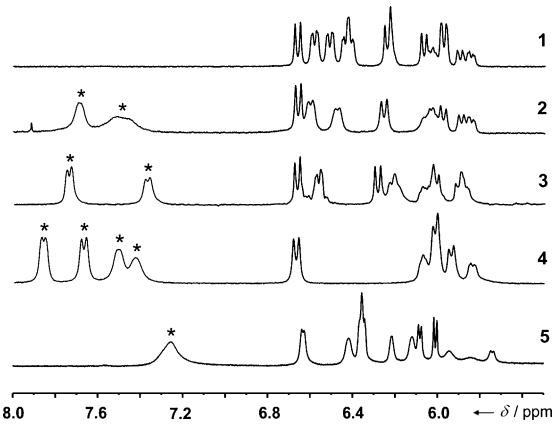

Figure 2. Region of the 400 MHz ^{1}H NMR spectra of oligomers **1**–**5** in CD_3OH (5×10^{-3} M) at 298 K, showing the thiourea (annotated with a star) and urea (signals from 6.8 to 5 ppm) resonances.

We have previously highlighted that when placed in an helical environment the α-methylene protons of chiral diamine units exhibit a high degree of anisochronicity (δ splitting) with a difference of chemical shifts between α1 and α2 ($\Delta\delta$) reaching values above 1 ppm for the central residues.[18e,33] The $\Delta\delta$ values have been measured for each hexamer **1**–**5** and are listed in Table 2. Thiourea moieties locally modify the chemical environment of the backbone α-methylene protons, thus calling for caution when comparing the $\Delta\delta$ values of oligoureas and oligo(urea/thiourea) hybrids. Nevertheless, the $\Delta\delta$ values for the urea residues 3–6 in compounds **1** and **2** were found to adopt almost identical values (all >1 ppm) suggesting little influence of the thiourea units on the magnetic environment of these protons in compound **2**. The α-methylene protons of the thiourea units in oligomer **2** also exhibit a high degree of anisochronicity. Whereas the $\Delta\delta$ value of the first residue (Leu^{X1}) is almost unchanged between compounds **1** and **2** (0.93 for 0.96 ppm), the $\Delta\delta$ value of the second residue (Ala^{X2})

Table 2. The $\Delta\delta$ values (in [ppm]) measured for the backbone $^{\alpha}CH_2$ protons along the sequence in oligourea **1** and the related hybrids **2**–**6**.

Compd.	Val^{X6}	Ala^{u5}	Leu^{X4}	Val^{X3}	Ala^{X2}	Leu^{X1}
1	1.08	1.27	1.34	1.25	1.22	0.96
2	1.08	1.28	1.33	1.22	1.59	1.01
3	1.05	1.24	1.30	1.71	0.96	0.45
4	1.06	1.23	1.71	1.67	0.62	0.30
5	0.95	0.90	1.2	1.17	1.20	0.97
6	0.93	0.80	1.15	1.11	1.18	0.93

is increased by approximately 0.4 ppm in compound **2**. Overall these observations support the view that the replacement of urea NHs close to the negative end of the helix dipole (residues 1 and 2) by the more acidic thiourea NHs has only a limited influence on the intramolecular hydrogen-bonding scheme and the helix geometry. At first sight, the insertion of a thiourea bond at the third position of compound **3** (Val^{t3}) produced similar effects, that is, a high degree of anisochronicity of backbone $^{\alpha}CH_2$ protons in the thiourea unit ($+0.49$ ppm compared to the $\Delta\delta$ value measured in hexamer **1**) and almost no variation of the $\Delta\delta$ values for residues following the thiourea unit (positions 4–6) compared to compound **1**. However, the $\Delta\delta$ value for the first residue in compound **3** (Leu^{u1}) is reduced by half, which may suggest a weakened hydrogen-bonding interaction between the first oxo-urea NHs and the C=S group at the *i*+2 position. This trend is amplified when two consecutive thiourea bonds are inserted in the middle of the sequence as in hybrid **4.** The α-methylene protons of the first two residues in compound **4** display markedly reduced $\Delta\delta$ values compared to hexamer **1** (≈ -0.6 ppm for both), thus reflecting a modified geometry and/or increased dynamics at this helix end.

The introduction of a thiourea unit at the last position (i.e., compound **5)** has a comparatively more limited effect on the $\Delta\delta$ value of the backbone methylene protons at the $i-2$ position (≈ -0.14 ppm) and thus provides some evidence that only minor adjustments are taking place in this part of the helix. Instead, anisochronicity of the methylene protons of the penultimate residue is significantly reduced (≈ -0.37 ppm) suggesting a possible perturbation of the first hydrogen-bonding interaction between the carbonyl group of the Boc group and the NHs of the urea between residues 3 and 4.

Additional insight into the conformations of urea/thiourea hybrid oligomers **2**–**5** was obtained by inspection of non-sequential rOe crosspeaks extracted from the ROESY experiments at 298 K and comparison with the homooligourea **1** (Figures S48 and S49 and Tables S8–S12 in the Supporting Information). Helical homooligoureas are characterized by a typical rOe pattern with medium-range connectivities of the type $^{\beta}CH(i+2)/N'H(i)$, $^{\beta}CH(i+2)/NH(i)$, and also $^{\alpha}CH(i+2)/N'H(i)$.[18c–e, 33a] This rOe pattern was observed in hexamer **1** although some resonance overlaps precluded unambiguous identification of rOe connectivities involving NHMe and NH groups of Leu^{u1}. Specific CH_3(Boc)/NH(4), CH_3(Boc)/N'H(5), and CH_3(Boc)/NH(5) connectivities were a good indicator of terminal helical folding (Figure S49 in the Supporting Information). In general, rOe connectivities of thiourea NHs in hybrid oligomers were more difficult to detect and assign due to line-broadening effects. Nevertheless, a very similar rOe pattern including a terminal CH_3(Boc)/N'H(5) rOe was observed in compounds **2** and **3**, strongly supporting a helical conformation (see Figure S49 in the Supporting Information). A lower number of medium range rOe connectivities indicative of helix formation were observed in compounds **4** and **5**. In both cases, the absence of medium range rOe crosspeaks with CH_3(Boc) may suggest terminal helix fraying resulting from the absence of a well-defined conformation at the end of the sequence.

Finally, to gain information at atomic resolution about the structural consequences of inserting discrete thiourea bonds, we examined the possibility to grow crystals of compound **1** and hybrids **2**–**5** for crystallographic studies. We obtained single crystals of oligomers **1**–**3** and **5** suitable for X-ray diffraction studies but our attempts to grow crystals of hybrid oligomer **4** remained unsuccessful. The structure of compound **1** was solved in the triclinic *P*1 space group and that of hybrids **2**, **3**, and **5** in the monoclinic $P2_1$ space group. The asymmetric units (ASUs) of crystals of compounds **3** and **5** were found to contain two and three independent molecules, respectively. As shown in Figure 3, the structures of compounds **2**, **3**(I), and **5**(I) are all helical and compare well with the canonical helix of homooligourea **1**. The introduction of two thioureas at the first two positions in the sequence has very limited influence on the overall helix geometry, which is in agreement with solution studies. An overlay of the structures of hexamers **1** and **2**, by fitting the six pairs of β-carbon atoms confirm the very close match between the two structures (root mean-square deviation values (RMSD) of 0.20 Å, see Figure S52 in the Supporting Information), the two thiocarbonyl groups in compound **2** pointing towards the solvent.

Conversely, examination of the structures of oligomers **3** and **5** reveals that the helical backbone rearranges locally to allow the formation of intramolecular hydrogen bonds between the C=S and the urea NH groups. One consequence is possibly a higher flexibility as reflected by the structural differences between the independent molecules in the corresponding ASUs. The C=S···HN bond parameters in these structures are collected in Table S14 in the Supporting Information. The S···N distance was found to vary between 3.23 and 3.56 Å and the C=S···H bond angle between 104 and 174° (mean values of the corresponding O···N bond length and C=O···H angle in hexamer **1** are 2.91 Å and 148°, respectively). Overlay of the structure of molecules **1**, **3**(I), and **3**(II) reveals that the C=S overlaps the canonical C=O position and that the rest of the chain fluctuates to place the urea NHs within an hydrogen-bonded distance (Figure 3b). This structural variability in oligomer **3**, which essentially concerns the last residue close to the negative pole of the helix is supported by decreased methylene anisochronicity at that position compared to hexamer **1** (see Table 1). This helical arrangement is largely maintained in **13**, a shorter analogue of **3** with benzyl side chains (see the Supporting Information for its synthesis). An overlay of molecules **3**(I) and **13**(I) is shown in Figure 3c (RMSD = 0.37 Å calculated over five pairs of β-carbon atoms).

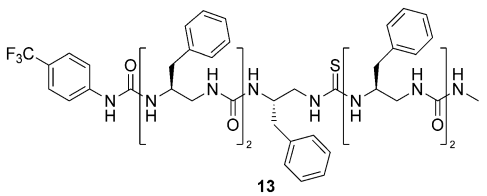

13

Alternatively, the C=S moiety in compound **5** can adopt an orientation different from that of the C=O moiety in compound **1** to maximize the C=S···H–N bond angle and length

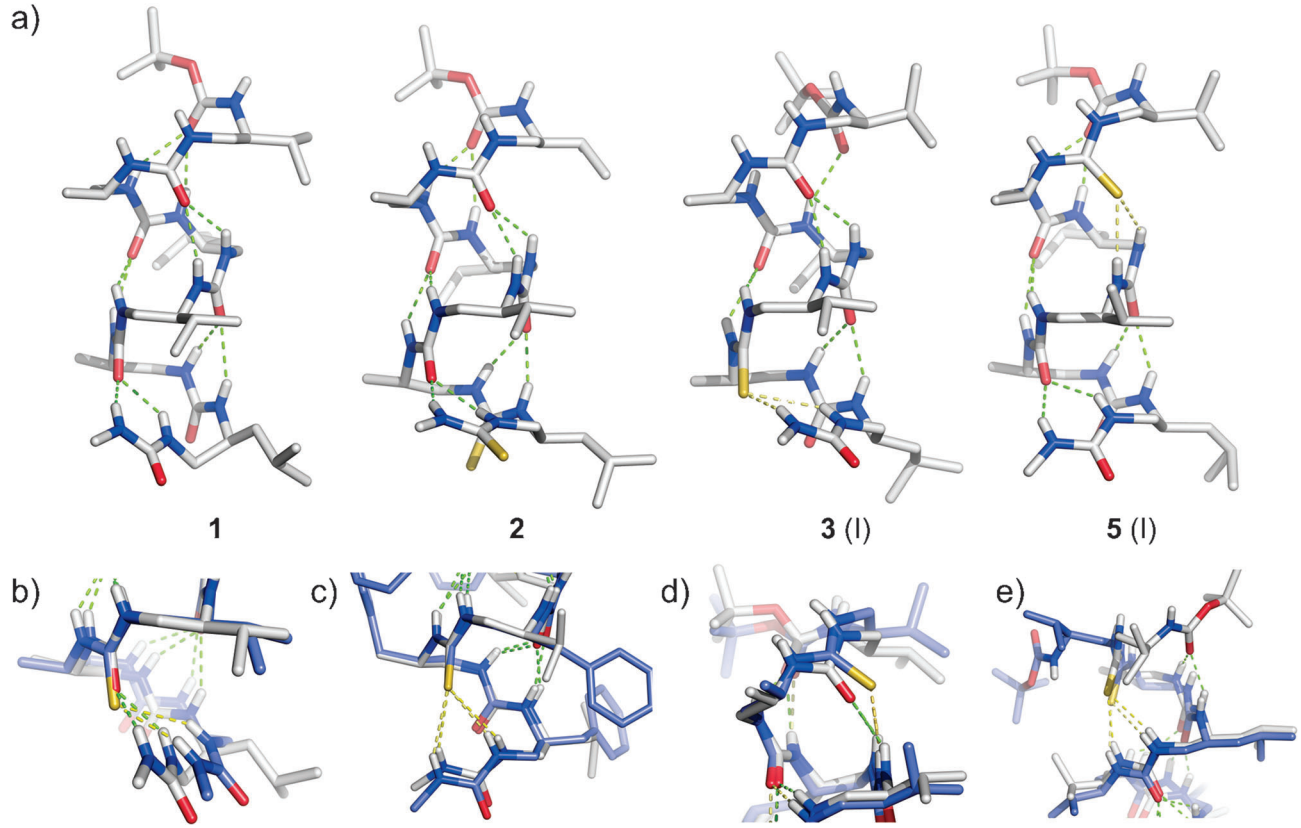

Figure 3. a) Comparison of the structures of oligoureas **1**, **2**, **3**, and **5** in the crystalline state. Only one of the two and three independent molecules present in the ASUs are shown for compounds **3** and **5**, respectively. b) Overlay of the structures of oligomers **1** and **3**(I) showing the slight conformational rearrangement caused by thiourea hydrogen bonding at the negative pole of the helix. c) Overlay of hybrids **3**(II) and **13**(I) showing little backbone deviation upon sequence variation. Carbon atoms in **3**(II) and **13**(I) are depicted in white and slate blue, respectively. d) Overlay of the structures of molecules **1** and **5**(I) highlighting the different hydrogen-bonded orientation of the penultimate backbone urea C=O and thiourea C=S groups, respectively. Carbon atoms in molecules **1** and **5**(I) are depicted in white and slate blue, respectively. e) Overlay of the two independent molecules **5**(I) and **5**(II) showing partial helix unwinding in **5**(II) and the loss of the terminal hydrogen bond involving the carbonyl group of the Boc group.

(Figure 3d). This is obtained through a concerted increase of both the φ and θ_2 backbone dihedral angles in Ala^{u5}. The possible consequence of this local rearrangement in oligomer **5**, that is, an increased flexibility of the helix terminus, becomes apparent when examining the structural differences between independent molecules in the ASU (see overlay of molecules **3**(I) and **3**(II) in Figure 3e). Whereas the structure of **3**(I) is fully helical, the structures of **3**(II) and **3**(III) are characterized by a 180° flip of the terminal atoms around the $^{\alpha}$C–N′ bond of Val^{t6} ($\theta_2 = +76.3°$ in **3**(I) but $-97.6°$ in **3**(II)) causing a loss of the terminal hydrogen bond with the Boc carbonyl group. This case of partial helix unwinding has some similarity with that previously documented for urea/carbamate oligomers in which carbamate units although compatible with a helical geometry tend to partly destabilize the helical conformation of oligoureas.[34]

Folding propensity of homooligothioureas

As shown above, the insertion of discrete thiourea bonds in the backbone of a urea-based foldamer has different outcome but does not generally compromise the formation of a helical structure in solution and in the solid state even though it is likely associated with an increased conformational flexibility. To further explore the behavior of backbones with thiourea units, we have synthesized and studied compound **7**, a homooligomer containing exclusively thiourea linkages.

The ECD spectrum of oligothiourea **7** reveals a distinct signature with a negative band at 242 nm, a stronger maximum of positive molar ellipticity at around 225 nm, a shoulder at 204 nm and a weak negative band at 188 nm (Figure 4a). Whereas the band at 225 nm was observed in all hybrids, the band at 242 nm was hardly visible in the spectra of hybrids **2**–**5**. To possibly correlate this ECD signature with a folding behavior, we have evaluated the chain length dependence in this series. The ECD spectra of shorter *N*-Boc-protected oligomers **14**–**18** ranging from one to five thiourea units (see the Supporting Information for the formulae) have been recorded under similar conditions. Although the intensity of the CD signal vary with the length of the oligomer (Figure 4a), the mean residue ellipticity (MRE) values of the negative and positive maxima at 242 and 225 nm do not exhibit chain length dependence (Figure 4a, inset). This observation is in sharp contrast to helical homooligoureas,[18d] and rather supports the absence of a cooperative folding process based on long-range interactions in hexathiourea **7**.

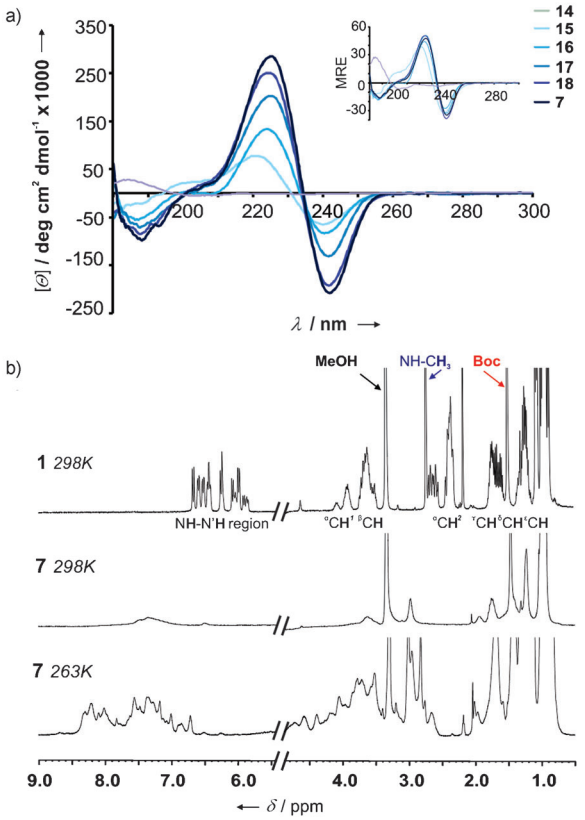

Figure 4. Spectroscopic characterization of thiourea homooligomer **7**. a) ECD spectra of compound **7** and the shorter analogues **14**–**18** recorded in TFE (2×10^{-4} M) at 298 K. Inset: Conversion to mean residue ellipticity (MRE). b) Overlay of the ^{1}H NMR spectra of compound **7** recorded at 298 and 263 K in CD_3OH (5×10^{-3} M) with that of oligourea **1** recorded at 298 K in the same solvent.

The NMR investigation of oligomer **7** failed to provide further evidence of a defined folded structure. The ^{1}H NMR spectrum of compound **7** recorded in CD_3OH at room temperature is poorly resolved compared to oligomer **1** and the sequence assignment was hampered by severe peak broadening and resonance overlaps (Figure 4 b). Line broadening is likely due to *Z*–*E* rotameric interconversion about the C–N bonds of the thioureas. The C–N rotation barriers in the thioureas have been experimentally determined, with $\Delta G^{\neq}$ values in the range of 11–14 kcal mol^{-1} slightly above that of ureas.[32] Although rotation remains too fast at room temperature for the peaks to separate, evidence for rotameric equilibrium is supported by variable-temperature experiments conducted on oligomer **7**. As the temperature is lowered, the resonances for possible *Z*–*E* conformers start to separate. A considerably more complex ^{1}H NMR spectrum with sharper resonances was measured at 263 K that reflects the multiple conformations resulting from *Z*–*E* isomerism around the six thiourea linkages in the molecule (Figure 4 b).[35,36]

Selenourea at the penultimate position cause partial helix unfolding

X-ray structure analysis of crystals of hybrid hexamer **5**, which contains an oxo to thiooxo replacement at the penultimate position has revealed two different conformational states of the molecule, either fully helical or partly unfolded (see above). Herein, we set out to extend the unfolded region observed in molecules **5**(II) and **5**(III) by applying a selenoxo substitution. We reasoned that the replacement of sulfur by selenium [larger van der Waals radius (r_{VDW}(Se) = 1.90 Å),[37] increased atomic polarizability compared to sulfur, longer C=Se bond length ($d_{C=Se}$ in selenourea derivatives ≈1.85 Å[38])] would more significantly hamper the propagation of the canonical hydrogen-bonding scheme of oligoureas, thus leading to an increased main chain disorganization.

The ECD characterization of oligomer **6** in TFE revealed a signature similar to that of compound **5** albeit with a weaker intensity, with bands at 188 (negative), 203 (positive), and a positive shoulder around 225 nm values, which may suggest helical folding, at least partly (Figure 5). The ^{1}H NMR spectrum

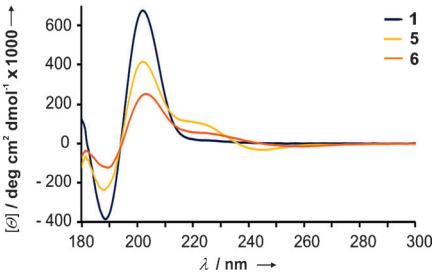

Figure 5. ECD spectra of oligomers **1**, **5**, and **6** in TFE (2×10^{-4} M) and 298 K.

of compound **6** recorded at 298 K was moderately informative for detailed conformational investigation due to a resonance broadening effect of the NH signals that was even more pronounced than with the thioureas (see the Supporting Information), which is in agreement with previous observations.[10] However, the anisochronicity values of the backbone methylene protons match those found in hybrid **5** for all residues, thus suggesting some similarity between the two structures, including conformational variability at the helix terminus (see Table S6 in the Supporting Information).

We were able to grow single crystals of compound **6** in MeCN/DMSO (95:5, v/v) and the structure was solved in the $P2_12_12_1$ space group. The crystal structure is notable among helical foldamers for the coexistence of a well-defined helical segment with a fragment that is largely unfolded (Figure 6). The mean backbone torsion angles measured on the first four residues match well those adopted by helically folded oligourea **1** (RMSD = 0.425 Å). Whereas the three centered hydrogen bonds between the C=X(6) and urea N'H(3) and NH(4) is present in the structures of oligomers **1** (X = O) and **5** (X = S), it is not supported by selenoxo substitution (X = Se) and the helicity of compound **6** is lost following the $^{\alpha}$C of residue five (Ala^{u5}) with large structural deviation for the unwound region.

The backbone dihedral angles of Ala^{u5} in the structure of compound **6** are collected in Table 3 together with those of oligomers **1** and **5**(I)–**5**(III) for comparison. Whereas the Φ angle of this residue 5 (but also for residue 6) is close to that

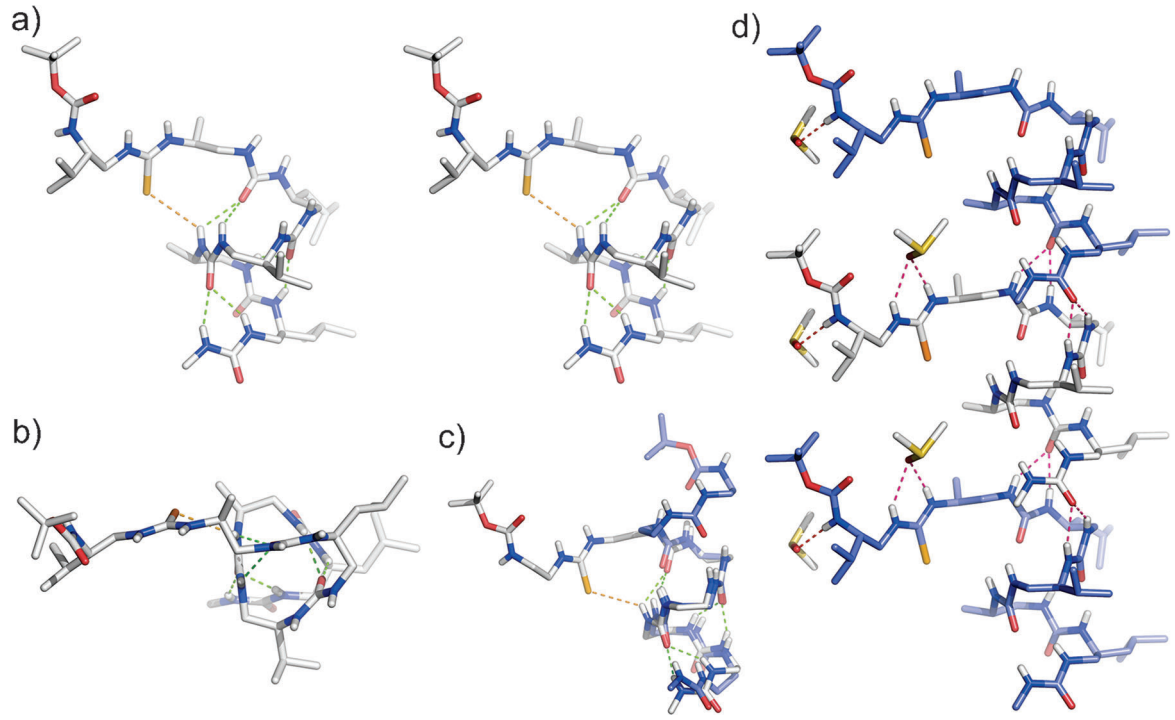

Figure 6. Crystal structure of the selenourea/urea hybrid oligomer **6** showing the coexistence of helically folded and unfolded segments. a) Stereoview along the helix axis. b) Topview. c) Overlay with the structure of homooligourea **1** (carbon atoms in slate blue). Side chains have been omitted for clarity. d) Packing of the oligomers and the hydrogen-bonded DMSO molecules in the crystal structure of oligomer **6**. Intermolecular hydrogen bonds are shown in magenta.

Table 3. Comparison of the main backbone torsion angles (in [°]) for the Ala^{u5} unit in the crystal structures of compounds **1**, **5**, and **6**.

	1	**5**[a]	**6**
Φ	−92	−108	−105
θ_1	54	57	−176
θ_2	84	84	−87

[a] Mean angles from the three independent molecules I–III in the ASU.

found in the oligourea helices, the θ_1 and θ_2 angles at these two residues considerably diverge from that canonical values; residue 5 adopting an *anti* conformation about the $^{\alpha}C$–$^{\beta}C$ bond ($\theta_1 = -176^{\circ}$). It is noteworthy that the selenocarbonyl ($d_{C-Se} = 1.88$ Å), which is oriented parallel to the helix axis is actually hydrogen bonded to the NH of Ala^{u2} ($d_{Se-N} = 3.75$ Å; C=Se···H bond angle = 120°) thus possibly stabilizing this unusual extended conformation of the backbone. The helical segments in the crystal structure of oligomer **6** are packed end-to-end in a columnar arrangement similar to what is generally observed for fully helical oligoureas; the carbonyl groups of the first two residues forming a hydrogen bond with the solvent-oriented NH groups of a second molecule (Figure 6d). Two well-defined DMSO molecules are hydrogen bonded to the carbamate and selenourea NHs in the partly unfolded and thus solvent-exposed part of the molecule (Figure 6d).

Conclusion

The replacement of the amide bond by the conservative thioxoamide in the peptide backbone is a well appreciated approach to study hydrogen-bond formation and folding among α-peptides,[6] proteins,[7] and oligoamide foldamers.[13,14] It also provides a versatile mean to increase the resistance of α-peptides to proteolysis,[39] and to modulate the receptor selectivity and affinity.[5a,c] In the present study, we show that the modification of the main chain of aliphatic *N*,*N*′-linked urea oligomers by isosteric oxo to thioxo replacements at selected positions in the sequence (positional thiourea scan) can also provide unique information about the folding process and intramolecular hydrogen bonding in this family of peptidomimetic helical foldamers. The differential hydrogen-bonding properties of thioureas relative to ureas, that is, an increased hydrogen-bond donor but lower hydrogen-bond acceptor capacity together with the increased C=X bond length impact on the oligourea helical folding to various degrees depending on the position of the substitution in the sequence. Whereas two adjacent thiooxo replacements at the negative end of the helix dipole (residues 1 and 2 in compound **2**) strongly promote canonical helix formation (the C=S moieties point towards the solvent), the same modification in the central part of the sequence (i.e., compound **4**) significantly affects the helix folding propensity of the preceding residues. Crystallographic studies of monosubstituted oligomers show that the helical backbone tends to rearrange upon formation of intramolecular C=S···HN bonds. This local rearrangement may increase the conforma-

tional flexibility and cause helix fraying as in the structures of molecules **5**(II) and **5**(III). Increasing further the C=X bond length by using a selenoxo substitution results in the loss of the canonical intrahelical C=X···HN hydrogen bond and in increased main chain disorganization. In this respect, the X-ray structure of the urea/selenourea hybrid **6**, which can be described as partly folded with a short canonical helical segment juxtaposed with a solvent exposed, elongated strand, is noteworthy. Although frayed-end helices[34,40] and bent helical conformations[41] are not uncommon among foldamer crystal structures, conformations in which a long-range order is compromised have been less frequently characterized at atomic resolution.[42]

The folding propensity of aliphatic homooligomers made exclusively of thiourea units was investigated for the first time. In contrast to the cognate urea oligomers, there is no spectroscopic evidence that homooligothioureas adopt defined folded conformations stabilized by remote hydrogen bonds. However, a conformational equilibrium between multiple thiourea *Z–E* conformers was revealed by low-temperature experiments, thus suggesting that at least partly folded hydrogen-bonded states might nevertheless be populated.

Taken together, this and earlier work from our laboratory[24b] demonstrate that the helical backbone of aliphatic *N*,*N*′-bridged oligoureas is robust and largely permissive to isosteric backbone modifications: amide (NH→CH_2), carbamate (NH→O), thioxo (C=O→C=S), as long as the overall proportion of these isosteric units in the sequence remains below a certain threshold. By allowing helix parameters (geometry and polarity) to be tuned with precision, a positional thiourea scan may prove useful to study the interplay between folding, membrane interacting properties, and antibacterial activities of oligoureas mimicking host defense peptides.[43] The facile transformation of thioureas into guanidiniums[44] and the importance of this moiety in biology, medicinal chemistry, drug delivery, and supramolecular structures also suggests application of (thio)urea hybrid oligomers as synthetic intermediates towards the elaboration of oligomers incorporating *N*,*N*′-linked guanidinium units at selected positions in the main chain.[45] The synthesis, and exploration of the folding and chemical properties of these novel urea/guanidinium hybrid backbones will be reported in due course.

Experimental Section

General

Commercially available reagents were used throughout without purification. Thin layer chromatography (TLC) was performed on silica gel 60 F254 (Merck) with detection by UV light and charring with 1% ninhydrin in ethanol followed by heating. Flash column chromatography was carried out on silica gel (40–63 μm, Merck). ^{1}H NMR and ^{13}C NMR spectra were recorded on four different NMR spectrometers: 1) an Avance II NMR spectrometer (Bruker Biospin) with a vertical 7.05 T narrow-bore/ultrashield magnet operating at 300 MHz for ^{1}H observation and 75 MHz for ^{13}C observation by means of a 5 mm direct BBO 1H/19F XBB H probe with Z gradient capabilities, 2) a DPX-400 NMR spectrometer (Bruker Biospin) with an avertical 9.4 T narrow-bore/ultrashield magnet operating at 400 MHz for ^{1}H observation by means of a 5 mm direct QNP ^{1}H/^{13}C/^{31}P/^{19}F probe with gradient capabilities. 3) an Avance III NMR spectrometer (Bruker Biospin) with a vertical 16.45 T narrow-bore/ultrashield magnet operating at 700 MHz for ^{1}H observation by means of a 5 mm TXI ^{1}H/^{13}C/^{15}N probe with Z gradient capabilities, and 4) a standard bore Bruker Avance III spectrometer operating at 800.23 MHz for proton detection. Chemical shifts are reported in parts per million (ppm, δ) relative to the ^{1}H or ^{13}C residual signal of the deuterated solvent used. ^{1}H NMR splitting patterns with observed first-order coupling are designated as singlet (s), broad singlet (br s), doublet (d), triplet (t), or quartet (q). Coupling constants (*J*) are reported in Hertz. ESI-MS analyses were carried out on a Thermo Exactive from the Mass Spectrometry Laboratory at the European Institute of Chemistry and Biology (UMS 3033 - IECB), Pessac, France.

Activated (*S*)-succinimidyl-{2-{[(*tert*-butoxy)carbonyl]amino}-2-X-ethyl}carbamate monomers[24] for the introduction of urea bonds and (*S*)-*tert*-butyl 1-isoselenocyanato-3-methylbutan-2-ylcarbamate (**12**)[27] were prepared from *N*-Boc-protected ethylene diamine derivatives **8** using previously described procedures.

Synthesis of the activated thio-monomers 9a–c

(S)-tert-*butyl (1-(1*H*-benzo[d][1,2,3]triazole-1-carbothioamido)propan-2-yl)carbamate (**9a**)*: To a stirred solution of bis(benzotriazolyl)methanethione[25] (1.60 g, 5.74 mmol) in CH_2Cl_2 (20 mL) at 0 °C was added amine **8a** (1.0 g, 5.74 mmol) in CH_2Cl_2 (10 mL) and the reaction mixture was left under stirring for 24 h. After reaction completion, the solvent was evaporated and the crude residue was purified by silica gel column chromatography (elution: 30–35% EtOAc in cyclohexane) to afford compound **9a** (0.802 g, 42%) as an off white solid. $[\alpha]_D^{20} = +13.43$ ($c = 1.0$ in MeOH); ^{1}H NMR (300 MHz, $CDCl_3$): $\delta = 10.00$ (s, 1H), 8.90 (dd, $J = 5.0$, 4.2 Hz, 1H), 8.13–8.07 (m, 1H), 7.68–7.58 (m, 1H), 7.52–7.42 (m, 1H), 4.97–4.62 (m, 1H), 4.29–4.09 (m, 1H), 4.07–3.88 (m, 1H), 3.88–3.65 (m 1H), 1.44 (s, 9H), 1.33 ppm (d, $J = 6.8$ Hz, 3H); ^{13}C NMR (75 MHz, $CDCl_3$): $\delta = 175.0$, 156.4, 147.0, 132.4, 130.0, 125.5, 120.2, 116.0, 80.4, 52.2, 45.6, 28.2, 18.8 ppm; HRMS (ESI) *m/z* calcd for $C_{15}H_{21}N_5O_2SNa$ [M^++Na]: 358.13082; found: 358.13204.

(S)-tert-*butyl 1-(1*H*-benzo[d][1,2,3]triazole-1-carbothioamido)-3-methyl-butan-2-ylcarbamate (**9b**)*: To a stirred solution of bis(benzotriazolyl)methanethione[25] (0.681 g, 2.435 mmol) in CH_2Cl_2 (15 mL) at 0 °C was added amine **8b** (0.492 g, 2.435 mmol) in CH_2Cl_2 (10 mL) and the reaction mixture was left under stirring for 24 h. After reaction completion, the solvent was evaporated and the crude residue was purified by silica gel column chromatography (elution: 10% EtOAc in cyclohexane) to afford product **9b** (0.690 g, 78%) as an off white solid. $[\alpha]_D^{20} = -12.63$ ($c = 1.0$ in MeOH); ^{1}H NMR (300 MHz, $CDCl_3$): $\delta = 9.82$ (s, 1H), 8.95–8.87 (m, 1H), 8.14–8.05 (m, 1H) 7.68–7.59 (m, 1H), 7.52–7.49 (m, 1H), 4.73 (d, $J = 6.7$ Hz, 1H), 4.20–3.58 (m, 3H), 2.11–1.82 (m, 1H), 1.42 (s, 9H), 1.05 ppm (t, $J = 6.7$ Hz, 6H); ^{13}C NMR (75 MHz, $CDCl_3$): $\delta = 175.0$, 156.8, 147.0, 132.4, 130.0, 125.5, 120.2, 115.9, 80.3, 54.8, 49.0, 30.7, 28.2, 19.3, 18.3 ppm; HRMS (ESI) *m/z* calcd for $C_{17}H_{25}N_5O_2SNa$ [M^++Na]: 386.16212; found: 386.16274.

(S)-tert-*butyl 1-(1*H*-benzo[d][1,2,3]triazole-1-carbothioamido)-4-methyl-pentan-2-yl carbamate (**9c**)*: To a solution of bis(benzotriazolyl)methanethione[25] (0.829 g, 2.962 mmol) in CH_2Cl_2 (15 mL) at 0 °C was added amine **8c** (0.640 g, 2.962 mmol) in CH_2Cl_2 (10 mL) and the reaction mixture was left under stirring for 24 h. After reaction completion, the solvent was evaporated and the crude residue was purified by silica gel column chromatography (elution: 10% EtOAc

in cyclohexane) to afford product **9c** (0.870 g, 78%) as a solid. $[\alpha]_D^{20} = -11.17$ ($c = 1.0$ in MeOH); ^{1}H NMR (300 MHz, $CDCl_3$): $\delta = 9.94$ (s, 1H), 8.93 (d, $J = 8.5$ Hz, 1H), 8.12 (d, $J = 8.3$ Hz, 1H), 7.71–7.59 (m, 1H), 7.55–7.44 (m, 1H), 4.66–4.51 (m, 1H), 4.23–4.05 (m, 1H), 4.04–3.92 (m, 1H), 3.85–3.64 (m, 1H), 1.91–1.71 (m 1H), 1.56–1.41 (m, 2H), 1.44 (s, 9H), 0.99 ppm (dd, $J = 6.5$, 5.4 Hz, 6H); ^{13}C NMR (75 MHz, $CDCl_3$): $\delta = 175.4$, 157.0, 147.4, 132.8, 130.4, 125.9, 120.6, 116.4, 80.8, 51.9, 48.4, 42.4, 28.6, 25.2, 23.3, 22.4 ppm; HRMS (ESI) *m/z* calcd for $C_{18}H_{27}N_5O_2SNa$ [M^++Na]: 400.17777; found: 400.17860.

Synthesis of oligomers

Detailed experimental procedures for the preparation of oligourea **1**, the urea/thiourea hybrid oligomers **2**–**5** and **13**, the thiourea homooligomers **7** and **14**–**18**, and the urea/seleno urea hybrid oligomer **6** are reported in the Supporting Information.

Circular dichroism

CD spectra of all oligomers were recorded on a J-815 Jasco spectropolarimeter (Jasco France. Nantes. France). Data are expressed in terms of the total molar ellipticity (or mean residue ellipticity) in [deg cm^2 dmol^{-1}]. CD spectra of the oligomers (0.2 mM) were acquired in spectrograde trifluoroethanol between 180 and 300 nm by using a rectangular quartz cell with a path length of 1 mm (Hellma 110-QS 1 mm, Paris, France). To reduce the signal-to-noise ratio all spectra were recorded on an average of two consecutive scans.

FTIR spectroscopy

ATR-FTIR (attenuated total reflection) spectra were recorded with a Nicolet 6700 FT-IR spectrometer (Nicolet Instrument, Madison, WI) equipped with a mercury–cadmium–telluride detector cooled with liquid nitrogen at 77 K on a germanium crystal with mono-reflexion at room temperature.

X-ray diffraction studies

Data collections were performed on two different high-flux micro-focus Rigaku rotating anodes at the $Co_{K\alpha}$ wavelength. Data for compounds **1**, **2**, **6**, and **13** were collected on a micromax MM07 (800W) equipped with osmic Varimax mirrors and semi-cylindrical R-Axis spider IP detector. Data for compounds **3** and **5** were collected on a FRX (2.7kW) equipped with osmic Varimax mirrors and a Dectris Pilatus 200 K hybrid detector. The crystals were mounted on cryo-loops after quick soaking on Paratone-N oil from Hampton research and flash-frozen. Both diffractometers have partial chi geometry goniometer allowing omega-scan data collections. The data were processed with the CrystalClear suite version 1.36 and 2.1b25 (Rigaku/MSC, 2006). All crystal structures were solved by using direct methods implemented in SHELXD[46] and were refined by using the SHELXL 2013 version. Full-matrix least-squares refinements were performed on *F*2 for all unique reflections, minimizing $w(F_o^2 - F_c^2)^2$, with anisotropic displacement parameters for the non-hydrogen atoms. Hydrogen atoms were positioned in idealized positions and refined with a riding model, with U_{iso} constrained to 1.2 U_{eq} values of the parent atom (1.5 U_{eq} when CH_3). The positions and isotropic displacement parameters of the remaining hydrogen atoms were refined freely. SIMU and DELU commands were used to restrain some side chains as rigid groups and to restrain their displacement parameters. CCDC 1026125 (**1**), CCDC 1026127 (**2**), CCDC 1026128 (**3**), CCDC 1026143 (**5**), CCDC 1026129 (**6**), and CCDC 1026144 (**13**) contain the supplementary crystallographic data for this paper. These data can be obtained free of charge from The Cambridge Crystallographic Data Centre via www.ccdc.cam.ac.uk/data_request/cif.

Acknowledgements

This work was supported by the CNRS, the University of Bordeaux (UB), the Conseil Regional d'Aquitaine (Project #20091102003) and the Agence Nationale de la Recherche (ANR-10-RPDOC-016 and ANR-12-ASTR-0024). Fellowships from the University of Bordeaux (Y.R.N), from DGA and Région Aquitaine (S.A.) and ANR (A.S.) are gratefully acknowledged. The crystallographic data have been collected at the IECB X-ray facility (UMS3033 CNRS and UB, US001 INSERM). We thank Axelle Grélard and Estelle Morvan for their assistance with the NMR measurements.

Keywords: foldamers · helical structures · thioureas · unfolding · X-ray diffraction

[1] a) A. F. Spatola in *Chemistry and Biochemistry of Amino Acids, Peptides and Proteins, Vol. 7* (Ed.: B. Weinstein), Marcel Dekker, New York, **1983**, pp. 267–357; b) A. Choudhary, R. T. Raines, *ChemBioChem* **2011**, *12*, 1801–1807.

[2] a) V. N. Balaji, S. Profeta Jr, S. W. Dietrich, *Biochem. Biophys. Res. Commun.* **1987**, *145*, 834–841; b) T. T. Tran, A. W. Burgess, H. Treutlein, J. Perich, *J Pept. Res.* **2001**, *58*, 67–78.

[3] J. Helbing, H. Bregy, J. Bredenbeck, R. Pfister, P. Hamm, R. Huber, J. Wachtveitl, L. De Vico, M. Olivucci, *J. Am. Chem. Soc.* **2004**, *126*, 8823–8834.

[4] R. W. Newberry, B. VanVeller, I. A. Guzei, R. T. Raines, *J. Am. Chem. Soc.* **2013**, *135*, 7843–7846.

[5] a) D. B. Sherman, A. F. Spatola, W. S. Wire, T. F. Burks, T. M. D. Nguyen, P. W. Schiller, *Biochem. Biophys. Res. Commun.* **1989**, *162*, 1126–1132; b) P. Chen, J. Qu, *J. Org. Chem.* **2011**, *76*, 2994–3004; c) J. Xie, A. Okano, J. G. Pierce, R. C. James, S. Stamm, C. M. Crane, D. L. Boger, *J. Am. Chem. Soc.* **2012**, *134*, 1284–1297.

[6] a) M. Doi, S. Takehara, T. Ishida, M. Inoue, *Int. J. Pept. Protein Res.* **2009**, *34*, 369–373; b) J. Lehmann, A. Linden, H. Heimgartner, *Tetrahedron* **1998**, *54*, 8721–8736; c) J. H. Miwa, A. K. Patel, N. Vivatrat, S. M. Popek, A. M. Meyer, *Org. Lett.* **2001**, *3*, 3373–3375; d) J. H. Miwa, L. Pallivathucal, S. Gowda, K. E. Lee, *Org. Lett.* **2002**, *4*, 4655–4657; e) A. Reiner, D. Wildemann, G. Fischer, T. Kiefhaber, *J. Am. Chem. Soc.* **2008**, *130*, 8079–8084; f) R. M. Culik, H. Jo, W. F. DeGrado, F. Gai, *J. Am. Chem. Soc.* **2012**, *134*, 8026–8029.

[7] a) S. Batjargal, Y. J. Wang, J. M. Goldberg, R. F. Wissner, E. J. Petersson, *J. Am. Chem. Soc.* **2012**, *134*, 9172–9182; b) J. M. Goldberg, X. Chen, N. Meinhardt, D. C. Greenbaum, E. J. Petersson, *J. Am. Chem. Soc.* **2014**, *136*, 2086–2093.

[8] a) R. Frank, M. Jakob, F. Thunecke, G. Fischer, M. Schutkowski, *Angew. Chem. Int. Ed.* **2000**, *39*, 1120–1122; *Angew. Chem.* **2000**, *112*, 1163–1165; b) D. Wildemann, C. Schiene-Fischer, T. Aumüller, A. Bachmann, T. Kiefhaber, C. Lücke, G. Fischer, *J. Am. Chem. Soc.* **2007**, *129*, 4910–4918.

[9] M. De Poli, J. Clayden, *Org. Biomol. Chem.* **2014**, *12*, 836–843.

[10] Y. Huang, G. Jahreis, G. Fischer, C. Lücke, *Chem. Eur. J.* **2012**, *18*, 9841–9848.

[11] a) Y. Huang, G. Jahreis, C. Lücke, D. Wildemann, G. Fischer, *J. Am. Chem. Soc.* **2010**, *132*, 7578–7579; b) T. M. Vishwanatha, N. Narendra, B. Chattopadhyay, M. Mukherjee, V. V. Sureshbabu, *J. Org. Chem.* **2012**, *77*, 2689–2702.

[12] D. Seebach, A. K. Beck, D. J. Bierbaum, *Chem. Biodiversity* **2004**, *1*, 1111.

[13] a) T. Sifferlen, M. Rueping, K. Gademann, B. Jaun, D. Seebach, *Helv. Chim. Acta* **1999**, *82*, 2067–2093; b) Y. Otani, T. Hori, M. Kawahata, K. Yamaguchi, T. Ohwada, *Tetrahedron* **2012**, *68*, 4418–4428.

[14] a) B. C. Gorske, R. C. Nelson, Z. S. Bowden, T. A. Kufe, A. M. Childs, *J. Org. Chem.* **2013**, *78*, 11172 – 11183; b) J. S. Laursen, J. Engel-Andreasen, P. Fristrup, P. Harris, C. A. Olsen, *J. Am. Chem. Soc.* **2013**, *135*, 2835 – 2844.

[15] a) S. H. Gellman, *Acc. Chem. Res.* **1998**, *31*, 173 – 180; b) G. Guichard, I. Huc, *Chem. Commun.* **2011**, *47*, 5933 – 5941.

[16] K. Burgess, H. Shin, D. S. Linthicum, *Angew. Chem. Int. Ed. Engl.* **1995**, *34*, 907 – 909; *Angew. Chem.* **1995**, *107*, 975 – 977.

[17] L. Fischer, G. Guichard, *Org. Biomol. Chem.* **2010**, *8*, 3101 – 3117.

[18] a) N. Pendem, C. Douat, P. Claudon, M. Laguerre, S. Castano, B. Desbat, D. Cavagnat, E. Ennifar, B. Kauffmann, G. Guichard, *J. Am. Chem. Soc.* **2013**, *135*, 4884 – 4892; b) L. Fischer, P. Claudon, N. Pendem, E. Miclet, C. Didierjean, E. Ennifar, G. Guichard, *Angew. Chem. Int. Ed.* **2010**, *49*, 1067 – 1070; *Angew. Chem.* **2010**, *122*, 1085 – 1088; c) G. Guichard, A. Violette, G. Chassaing, E. Miclet, *Magn. Reson. Chem.* **2008**, *46*, 918 – 924; d) A. Violette, M. C. Averlant-Petit, V. Semetey, C. Hemmerlin, R. Casimir, R. Graff, M. Marraud, J.-P. Briand, D. Rognan, G. Guichard, *J. Am. Chem. Soc.* **2005**, *127*, 2156 – 2164; e) C. Hemmerlin, M. Marraud, D. Rognan, R. Graff, V. Semetey, J.-P. Briand, G. Guichard, *Helv. Chim. Acta* **2002**, *85*, 3692 – 3711.

[19] R. Custelcean, *Chem. Commun.* **2008**, 295 – 307.

[20] J. L. Sessler, P. A. Gale, W.-S. Cho, *Anion Receptor Chemistry*, RSC, Cambridge, **2006**.

[21] a) Y. Takemoto, *Org. Biomol. Chem.* **2005**, *3*, 4299 – 4306; b) Z. Zhang, P. R. Schreiner, *Chem. Soc. Rev.* **2009**, *38*, 1187 – 1198; c) S. J. Connon, *Chem. Eur. J.* **2006**, *12*, 5418 – 5427.

[22] a) F. G. Bordwell, J. C. Branca, D. L. Hughes, W. N. Olmstead, *J. Org. Chem.* **1980**, *45*, 3305 – 3313; b) G. Jakab, C. Tancon, Z. Zhang, K. M. Lippert, P. R. Schreiner, *Org. Lett.* **2012**, *14*, 1724 – 1727.

[23] a) F. H. Allen, C. M. Bird, R. S. Rowland, P. R. Raithby, *Acta Crystallogr. Sect. B* **1997**, *53*, 680 – 695; b) J. T. Lenthall, J. A. Foster, K. M. Anderson, M. R. Probert, J. A. K. Howard, J. W. Steed, *CrystEngComm* **2011**, *13*, 3202 – 3212.

[24] a) J. Fremaux, L. Fischer, T. Arbogast, B. Kauffmann, G. Guichard, *Angew. Chem. Int. Ed.* **2011**, *50*, 11382 – 11385; *Angew. Chem.* **2011**, *123*, 11584 – 11587; b) N. Pendem, Y. R. Nelli, C. Douat, L. Fischer, M. Laguerre, E. Ennifar, B. Kauffmann, G. Guichard, *Angew. Chem. Int. Ed.* **2013**, *52*, 4147 – 4151; *Angew. Chem.* **2013**, *125*, 4241 – 4245; c) G. Guichard, V. Semetey, C. Didierjean, A. Aubry, J.-P. Briand, M. Rodriguez, *J. Org. Chem.* **1999**, *64*, 8702 – 8705.

[25] A. R. Katritzky, D. P. M. Pleynet, B. Yang, *J. Org. Chem.* **1997**, *62*, 4155 – 4158.

[26] a) J. Smith, J. L. Liras, S. E. Schneider, E. V. Anslyn, *J. Org. Chem.* **1996**, *61*, 8811 – 8818; b) V. V. Sureshbabu, S. A. Naik, H. P. Hemantha, N. Narendra, U. Das, T. N. Guru Row, *J. Org. Chem.* **2009**, *74*, 5260 – 5266.

[27] a) G. Chennakrishnareddy, G. Nagendra, H. P. Hemantha, U. Das, T. N. Guru Row, V. V. Sureshbabu, *Tetrahedron* **2010**, *66*, 6718 – 6724.

[28] M. T. Oakley, G. Guichard, J. D. Hirst, *J. Phys. Chem. B* **2007**, *111*, 3274 – 3279.

[29] a) K. Rang, J. Sandström, C. Svensson, *Can. J. Chem.* **1998**, *76*, 811 – 820; b) J. Gawronski, M. Kwit, P. Skowronek, *Org. Biomol. Chem.* **2009**, *7*, 1562 – 1572.

[30] D. Cavagnat, P. Claudon, L. Fischer, G. Guichard, B. Desbat, *J. Phys. Chem. B* **2011**, *115*, 4446 – 4452.

[31] a) A. Yamaguchi, R. B. Penland, S. Mizushima, T. J. Lane, C. Curran, J. V. Quagliano, *J. Am. Chem. Soc.* **1958**, *80*, 527 – 529; b) K. Srinivasan, S. Gunasekaran, S. Krishnan, *Spectrochim. Acta Part A* **2010**, *75*, 1171 – 1175.

[32] a) M. L. Filleux-Blanchard, A. Durand, *Org. Magn. Reson.* **1971**, *3*, 187 – 191; b) K. A. Haushalter, J. Lau, J. D. Roberts, *J. Am. Chem. Soc.* **1996**, *118*, 8891 – 8896; c) C. O. Mellet, A. M. Marín, J. L. Jiménez Blanco, J. M. García Fernández, J. Fuentes, *Tetrahedron: Asymmetry* **1994**, *5*, 2325 – 2334.

[33] a) V. Semetey, D. Rognan, C. Hemmerlin, R. Graff, J.-P. Briand, M. Marraud, G. Guichard, *Angew. Chem. Int. Ed.* **2002**, *41*, 1893 – 1895; *Angew. Chem.* **2002**, *114*, 1973 – 1975; b) A. Violette, N. Lancelot, A. Poschalko, M. Piotto, J. P. Briand, J. Raya, K. Elbayed, A. Bianco, G. Guichard, *Chem. Eur. J.* **2008**, *14*, 3874 – 3882.

[34] Y. R. Nelli, L. Fischer, G. W. Collie, B. Kauffmann, G. Guichard, *Biopolymers* **2013**, *100*, 687 – 697.

[35] For detailed studies of *Z* – *E* isomerism equilibria in sugar thioureas and approaches aimed at controlling the folding in cognate bisureas, see also: J. L. Jiménez Blanco, J. M. Benito, C. O. Mellet, J. M. García Fernández, *Org. Lett.* **1999**, *1*, 1217 – 1220; D. Rodríguez-Lucena, J. M. Benito, C. O. Mellet, J. M. G. Fernandez, *Chem. Commun.* **2007**, 831 – 833.

[36] Urea *Z*–*E* interconversion has also been reported among aliphatic *N*,*N*′-linked urea oligomers, see : a) Reference [18d]; b) V. Semetey, C. Hemmerlin, C. Didierjean, A.-P. Schaffner, A. G. Giner, A. Aubry, J.-P. Briand, M. Marraud, G. Guichard, *Org. Lett.* **2001**, *3*, 3843 – 3846.

[37] A. Bondi, *J Phys. Chem.* **1964**, *68*, 441 – 451.

[38] a) J. S. Rutherford, C. Calvo, *Z. Kristallogr.* **1969**, *128*, 229; b) R. Gopal, B. E. Robertson, J. S. Rutherford, *Acta Crystallogr. Sect. C* **1989**, *45*, 257 – 259.

[39] a) K. L. Foje, R. P. Hanzlik, *Biochim. Biophys. Acta Gen. Subj.* **1994**, *1201*, 447 – 453; b) M. Schutkowski, K. Neubert, G. Fischer, *Eur. J. Biochem.* **1994**, *221*, 455 – 461; c) S. Yao, R. Zutshi, J. Chmielewski, *Bioorg. Med. Chem. Lett.* **1998**, *8*, 699 – 704.

[40] C. S. Hartley, J. He, *J. Org. Chem.* **2010**, *75*, 8627 – 8636.

[41] J. Fremaux, C. Dolain, B. Kauffmann, J. Clayden, G. Guichard, *Chem. Commun.* **2013**, *49*, 7415 – 7417.

[42] a) M. Kudo, V. Maurizot, H. Masu, A. Tanatani, I. Huc, *Chem. Commun.* **2014**, *50*, 10090 – 10093; b) L. Milli, M. Larocca, M. Tedesco, N. Castellucci, E. Ghibaudi, A. Cornia, M. Calvaresi, F. Zerbetto, C. Tomasini, *J. Org. Chem.* **2014**, *79*, 5958 – 5969.

[43] P. Claudon, A. Violette, K. Lamour, M. Decossas, S. Fournel, B. Heurtault, J. Godet, Y. Mély, B. Jamart-Grégoire, M.-C. Averlant-Petit, J.-P. Briand, G. Duportail, H. Monteil, G. Guichard, *Angew. Chem. Int. Ed.* **2010**, *49*, 333 – 336; *Angew. Chem.* **2010**, *122*, 343 – 346.

[44] a) C. R. Rasmussen, F. J. Villani Jr, B. E. Reynolds, J. N. Plampin, A. R. Hood, L. R. Hecker, S. O. Nortey, A. Hanslin, M. J. Costanzo, R. M. Howse Jr, A. J. Molinari, *Synthesis* **1988**, 460 – 466; b) J. C. Manimala, E. V. Anslyn, *Eur. J. Org. Chem.* **2002**, 3909 – 3922.

[45] a) A. Tanatani, H. Kagechika, I. Azumaya, R. Fukutomi, Y. Ito, K. Yamaguchi, K. Shudo, *Tetrahedron Lett.* **1997**, *38*, 4425 – 4428; b) S. E. Schneider, P. A. Bishop, M. A. Salazar, O. A. Bishop, E. V. Anslyn, *Tetrahedron* **1998**, *54*, 15063 – 15086; c) Z. Zhang, E. Fan, *J. Org. Chem.* **2005**, *70*, 8801 – 8810.

[46] G. Sheldrick, *Acta Crystallogr. Sect. A* **2008**, *64*, 112 – 122.

Received: October 23, 2014
Published online on December 21, 2014

